Parameters study on lateral buckling of submarine PIP pipelines

Xinhu Zhang[1,2a], Menglan Duan[*1,2], Yingying Wang[1,2b] and Tongtong Li[1,2c]

[1]*Offshore Oil and Gas Research Center, China University of Petroleum-Beijing, 18 Fuxue Road, Changping, Republic of China*
[2]*College of Mechanical and Transportation Engineering, China University of Petroleum-Beijing, 18 Fuxue Road, Changping, Republic of China*

Abstract. In meeting the technical needs for deepwater conditions and overcoming the shortfalls of single-layer pipes for deepwater applications, pipe-in-pipe (PIP) systems have been developed. While, for PIP pipelines directly laid on the seabed or with partial embedment, one of the primary service risks is lateral buckling. The critical axial force is a key factor governing the global lateral buckling response that has been paid much more attention. It is influenced by global imperfections, submerged weight, stiffness, pipe-soil interaction characteristics, et al. In this study, Finite Element Models for imperfect PIP systems are established on the basis of 3D beam element and tube-to-tube element in Abaqus. A parameter study was conducted to investigate the effects of these parameters on the critical axial force and post-buckling forms. These parameters include structural parameters such as imperfections, clearance, and bulkhead spacing, pipe/soil interaction parameter, for instance, axial and lateral friction properties between pipeline and seabed, and load parameter submerged weight. Python as a programming language is been used to realize parametric modeling in Abaqus. Some conclusions are obtained which can provide a guide for the design of PIP pipelines.

Keywords: lateral buckling; PIP; parameter analysis; numerical model

1. Introduction

With the development of offshore oil industry, offshore oil exploration has been going to marine deepwater gradually in recent years. In meeting the technical challenges for deepwater conditions and overcoming the shortfalls of single-layer pipes for deepwater applications, pipe-in-pipe (PIP) systems have been developed which stresses engineering design requirements with respect to flow assurance, transient, as well as serviceability and strength (DNV OS-F101 2012). While, for PIP pipelines directly laid on the seabed or with partial embedment, one of the primary service risks is lateral buckling. Pipelines with lateral buckling may lead to final failure such as collapse, fatigue or fracture *et al.* (DNV RP-F110 2007). So it is important to study this behavior.

∗Corresponding author, Professor, E-mail: mlduan@cup.edu.cn
[a] Ph.D. Student, E-mail: xinhu_zhang@126.com
[b] Lecture, E-mail: wyy5186@126.com
[c] Ph.D. Student, E-mail: dawntt1987@gmail.com

Many researchers have investigated the lateral buckling problem. Palmer and Baldry (1974) studied the lateral buckling of axially constrained pipelines by theoretical analysis and experiments. He correctly interpreted the reason why the pipe can buckle and obtained an analytical solution of the critical pressure. Hobbs (1984) studied lateral buckling phenomenon in perfect single-layer pipelines. He proposed that pipeline can buckle into different lateral modes. These lateral buckling modes can be divided into five types, as shown in Fig. 1. By solving the governing equation, he obtained five theoretical solutions corresponding to above five lateral buckling modes. Since then, a number of experimental and analytical studies on the lateral buckling of single-layer pipelines have been published, such as Taylor and Gan (1986), Taylor and Tran (1993), Taylor and Tran (1996). They mainly focused on the effect of initial imperfections on buckling response. Miles and Calladine (1999) proposed that initial lateral buckling is a localization phenomenon. They investigated these phenomena by means of a small–scale physical model and a computer simulation. The results from experiment and simulation are consistent. Simple formulas was been presented for the amplitude and wavelength of first formed lobe. Kershenbaum *et al.* (1996) proposed an analytical model for the lateral deviation of a single subsea pipeline due to thermal expansion. They applied energy method to determine the lateral deviation and natural wave lengths which are used to determine the pipeline sinusoidal shape, resultant pipeline stresses, and a more realistic pipeline expansion length. Plastic lateral resistance from soil friction is considered to have a small effect on the critical buckling loads. Soreide *et al.* (2005) applied analytical as well as numerical simulations to illustrate the different modes of deformation and design parameters of lateral buckling. The effects on allowable feed-in from soil resistance, pipeline weight and initial geometry are discussed in their analyses. Karampour and Albermani (2013) carried out analytical and numerical studies on lateral buckling of subsea pipelines. By comparing the results from theoretical analysis and numerical simulation, a new interpretation of localization is presented based on an isolated half-wavelength model. They obtained a conclusion that excessive bending stress can be induced under lateral buckling. Haq and Kenny (2013) presented a calibrated numerical modelling procedure. They mainly focused on the parameters study on lateral buckling of subsea pipelines. Above studies have focused on lateral buckling behavior only in single-layer pipelines. However, these researches provide a foundation for lateral buckling problem of PIP pipelines.
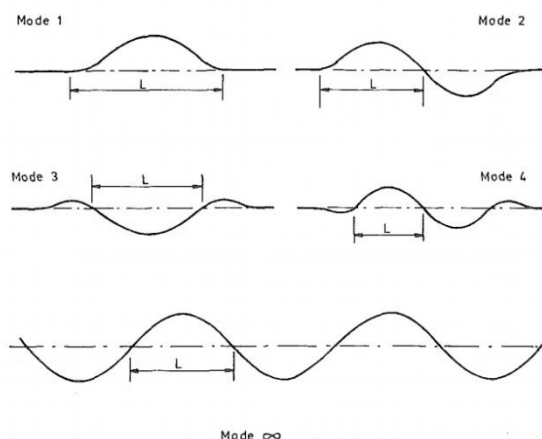

Fig. 1 Lateral buckling modes

Harrison *et al.* (1997) investigated the thermal expansion phenomenon in insulated PIP system. They presented an analytical method, investigation results and application of thermal expansion of subsea PIP system. In their analysis, temperature gradient, pressure, soil resistance, and interaction forces between inner pipe and outer pipe are considered. But they mainly focused on the calculation of pipe elongation, stresses and strains. Vaz and Patel (1999) presented an analytical formulation of the coupled buckling instability of a PIP system on the basis of beam theory. They found that the stiffness ratio of the inner and outer pipes as well as the number of centralizers affect the global buckling form in ideal PIP system. Whereas, because of they addressed the PIP buckling problem, the presence of seabed friction and the mutual constraint axial and rotational between the inner and outer pipes as well as initial imperfections are ignored. Zhao *et al.* (2007) investigated the lateral buckling process induced by high temperature using modified Risks method. Emphasis is placed on the acquiring a more precise description on PIP system buckling process by using Finite Element models. Haq and Kenny (2014) carried out numerical parameter study on later buckling response of subsea PIP pipeline. The parameters examined include pipe embedment, pipe out-of-straightness (OOS), soil shear strength, soil peak and residual forces and displacements, variation in soil properties distributed along the pipeline route, and external pressure associated with the installation depth. The observed pipe response was a complex relationship with these parameters and kinematic boundary conditions.

From above, we know that the lateral buckling response of PIP pipelines is a considerably complicated process. Many factors can affect the lateral buckling behavior of PIP system. Previous researches manifest that it is difficult to find an analytical solution considering adequate factors to describe the buckling performance of PIP systems. However, Finite Element Methods can be employed primarily to reveal the possible lateral buckling behavior for untrenched PIP systems.

In this study, Finite Element Models for imperfect PIP systems are established on the basis of 3D beam element and tube-to-tube element (ITT elements) in Abaqus. A parameter study is conducted to investigate the effects of these parameters including structural parameters such as imperfections, clearance, and bulkhead spacing, pipe/soil interaction parameter lateral friction property between pipeline and seabed, and load parameter submerged weight on the critical axial force and post-buckling forms. Python as a programming language is been used which can realize parametric modeling in Abaqus. Some conclusions are obtained which can provide a guide for the design of PIP pipelines. This paper will provide a foundation for future studies to establish engineering guidance on PIP Pipelines lateral buckling with respect to additional parameters including installation conditions and non-linear pipe/soil interaction characteristics *et al.*

2. Analysis method

2.1 Geometric model of PIP

In The basic configuration of a PIP pipeline is shown in Fig. 2. The PIP pipeline comprises inner pipe, outer pipe, thermal insulation material and a series of bulkheads and centralizers (Jukes *et al.* 2007). The inner pipe is used to convey the hydrocarbons and hence exposed to the internal pressure and temperature. The outer pipe is used to withstand the external pressure. The inner pipe and outer pipe are constrained by a series of centralizers. The centralizers are fixed with the inner pipe whereas the outer pipe is separated from the centralizers. So the inner pipe and the centralizers can move freely inside the outer pipe and transfer forces and displacements through

the contact between the centralizer and the outer pipe. In practice, the clearance between centralizers and outer pipe may be 1 mm-10 mm (Vaz *et al*. 1999) depending on the manufacturing precision. The annulus between inner and outer pipe is filled with dry insulation material. The end bulkhead is designed to connect the inner pipe to the outer pipe at each pipeline termination. Intermediate bulkheads may be required for reeled PIP to allow the top tension to be transferred between the outer pipe and the inner pipe.

2.2 Finite element model

According to the research of Palmer (1990), the finite element analysis is a convenient and effective tool to calculate the buckling of pipelines. The finite element model of the PIP system is described on the following five aspects.

2.2.1 Pipeline and seabed elements

In this study, the outer and inner pipes are modeled using the 3-dimensional 2-node linear Timoshenko beam element PIPE31 which can account transverse shear deformation and the effect of internal pressure and temperature. (ABAQUS 6.14 Analysis User's Guide 2014). The geometric parameters of inner and outer pipes are listed in Table 1. The outer and inner pipes are divided into 1200 equal length element respectively.
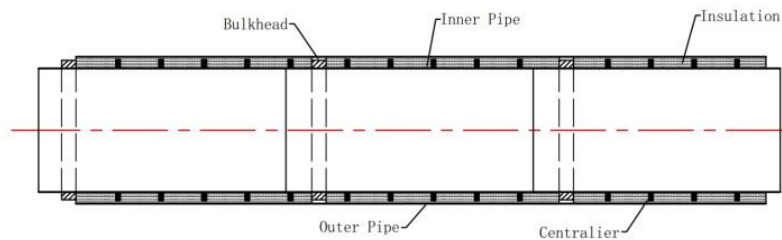

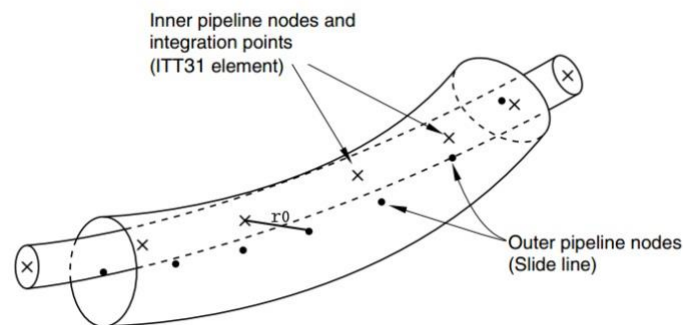
Fig. 2 Typical PIP configuration

Fig. 3 ITT31 element

Table 1 Geometric parameters of PIP pipeline

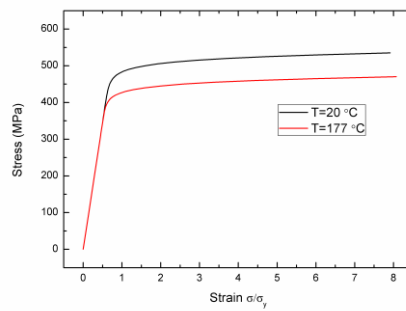| Parameters	Values	
	Inner pipe	Outer pipe
Length, m	1200	1200
Diameters	0.305	0.457
Thickness, m	0.02033	0.02285

Fig. 4 The stress-strain curve

The centralizer between the outer and inner pipes is modeled by 3-dimensional 1-node tube-to-tube contact element ITT31 which can model the finite-sliding interaction between two pipelines or tubes where one tube lies inside the other or between two tubes that lie next to each other (ABAQUS 6.14 Analysis User's Guide 2014). Hence, the ITT contact elements can accurately simulate the contact reaction forces and corresponding load transfer (through the centralizer) between the inner and the outer pipe. As shown in Fig. 3, ITT elements are attached to the node of the inner pipe. A slide line associated with the axial line of the outer pipe is needed to provide a path for ITT element. The key parameter r0 is used to describe the clearance between ITT elements and the outer pipe, as shown in Fig. 3.

The bulkheads are modeled by tie constraints for the corresponding nodes between the inner and outer pipes. In this study, in order to research the effects of bulkheads spacing on the lateral buckling response, bulkheads spacing are variable from 50 m to 1200 m.

The seabed is treated as a rigid foundation which is modeled using 3-dimensional 4-node discrete rigid element R3D4. In the research of Haq (2014), the elements with a size of 8 m×6 m are adopted. But a mesh topology study was carried out which manifested that the elements with a size of 20 m×20 m is enough. So in this study, we adopt the latter size.

2.2.2 Pipeline material properties

The pipeline material grade 483MPa (X70) is selected for both inner and outer pipes. The stress-strain curve is fitted with the Ramberg-Osgood model (Haq 2014, He 2014) defined as follows

$$\varepsilon = \frac{\sigma}{E}\left(1 + \frac{3}{7}(\frac{\sigma}{\sigma_y})^{n-1}\right)$$

$$(1)$$

According to the study of Haq (2014), the pipe material properties related to temperature are listed in Table 2. The stress-strain relationships are shown in Fig. 4. Apparently, with the increasing of temperature, the strength is decreased. Using linear interpolation method, the material properties corresponding to other temperature are obtained. In this study, the stress-strain relationship is defined as a piecewise nonlinear dataset with plastic material behavior defined by the von Mises yield criterion with isotropic hardening.

2.2.3 Pipe/Soil interaction

As mentioned before, the seabed is modeled as rigid surface. The Coulomb friction model with isotropic property is used to model the interface contact between the pipe and seabed. While, in researching the effect of friction on the lateral buckling, that model with anisotropic properties is been adopted. According to Rong *et al*. (2009), the best estimate defining the pipe breakout axial and lateral friction was 0.6 and 0.8, respectively. We make the axial friction coefficient be a constant 0.6 and the lateral friction coefficient varying from 0 to 1.2.

2.2.4 Loads and boundary conditions

The loads include the PIP submerged weight, internal and external pressure, operating and ambient temperature. The PIP submerged weight is modeled by downward forces per unit which is identical and evenly distributed linear loads with its value varying form 1500 N/m to 10500 N/m. The ambient seawater temperature and operating temperature is set as 20℃ and 177℃, respectively.

In the first load step, the initial conditions are defined that including the ambient seawater temperature and linear loads due to the submerged pipe weight. In the second load step, the external and internal pressure loads, and operating temperature are defined.

In the entire simulation, the ends of inner and outer pipe are fixed in X, Y and Z direction including three translational degrees of freedom and three rotational degrees of freedom.

2.2.5 Initial imperfection

In this study, one symmetric full-contact imperfection profile function is selected to account for undulations of the seabed. The function is (Karampour 2013, Zhang 2015)

Table 2 Pipe Material Properties

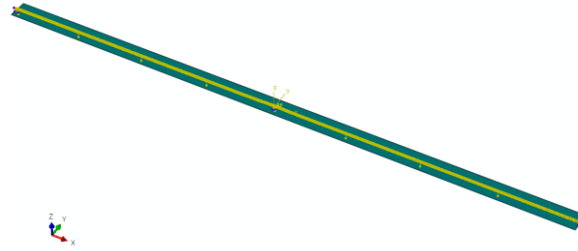| Parameters	Temperature	
	20℃	177℃
Young's modulus, GPa	207	206
Density, kg/m3	7850	7850
SMYS, MPa	483	422
SMTS, MPa	570	499
Poisson's ratio	0.3	0.3
Coefficient of thermal expansion, ℃-1	1.17E-5	1.31E-5

Fig. 5 The Finite Element Model of PIP pipeline

$$f_2(x) = \frac{w_0}{2}(1+\cos(\frac{2\pi x}{L_0})) \quad -\frac{L_0}{2} \le x \le \frac{L_0}{2}$$

(2)

Where w0 and L0 denote maximum height and wave length of imperfection, respectively. Hence w0/L0 denotes the out-of-straight (OOS) of pipelines. In this study in order to research the effect of OOS on lateral buckling response, we set w0 varying from 0.1 m to 3 m.

Finally the Finite Element Model is established, as shown in Fig. 5. In the next section, we will use this model to conduct parameter study.

2.3 Calculation method

The lateral buckling of PIP system is an unstable nonlinear and localized problem. Therefore, a local transfer of strain energy occurs from one part of the model to near parts. Pure Newton-Raphson method may lead to the problem of convergence difficulty. Additional an automatic stabilization method specifying dissipated energy fraction has been used for solving this nonlinear equilibrium problem.

3. Parameter study

From previous researches, we know that the buckling behaviors of PIP pipelines are affected by these factors, namely submerged weight Q, pipeline stiffness ratio β (as shown in Eq. (3)), pipeline initial imperfections OOS, lateral friction coefficient μ, clearance c between inner and outer pipe *et al*. In this study, we keep the diameters and wall thickness of inner pipe and outer pipe constants. So the stiffness ratio β is a constant 0.2514.

$$\beta = \frac{EI_{inner}}{EI_{outer}}$$

(3)

According to previous research Vaz (1999), Jukes (2009), sinusoidal buckling or helical buckling won't happen when the stiffness ratio take this value. We mainly study the effects of rest parameters Q, OOS, μ, c, and an additional parameter bulkhead spacing h on the later buckling critical force and bucked forms of PIP system. The range of these parameters is listed in Table 3.

Table 3 Parameter range

Parameter	Values							
Submerged weight Q (kN/m)	1500	3000	4500	6000	7500	9000	10500	-
OOS	0.001	0.002	0.005	0.008	0.01	0.015	0.02	0.03
Lateral friction coefficient μ	0	0.2	0.4	0.6	0.8	1.0	1.2	-
Clearance c (m)	0.001	0.002	0.005	0.008	0.016	0.024	0.032	0.048
Bulkhead spacing h (m)	50	100	200	300	400	600	1200	-

Totally, more than 2000 finite element models are performed.

Python, the programming language within the ABAQUS is used to create and manage the parametric study's files. The results are also processed by Python because of amazing amount of data. The results will be discussed in nest section.

4. Results and discussion

The lateral buckling behaviors of PIP pipelines have been simulated successfully. As shown in Fig. 6, when the temperature reach to 177℃, a typical contour of the axial stress and displacement of PIP pipelines are plotted. Apparently, the lateral buckling of PIP pipelines occurred. The effect of different factors on the lateral buckling critical force and buckled forms of PIP system will be analyzed in this section.

4.1 Influence of submerged weights

The lateral buckling response of PIP pipelines with different submerged weight Q is shown in Fig. 7. From Fig. 7(a) we know that a heavier submerged weight correspondents to a more evident of the "snap through" phenomenon and a higher critical temperature. When the submerged weight is over 9000 N/m, the maximum lateral displacement almost doesn't change. According to the critical temperature, the critical axial force is calculated as follows (Hobbs 1984)

$$F_c = EA\alpha\Delta T$$

(4)

The critical temperature and critical force are listed in Table 4. From Table 4, we know that the submerged weight varying from 1500 N/m to 10500 N/m, the critical force changes corresponding from 1.03E+6 to 5.23E+6. Therefore, the submerged weight significantly influences the critical force.

The post-buckling form is shown in Fig. 7(b). From this figure, it is clearly that the buckling modes (the number of wave in buckled region) are not change when the submerged weight varying from 1500 N/m to 10500 N/m. This buckling mode has five half-wave and is developed from Mode 3 Hobbs (1984) presented, as shown in Fig.1.
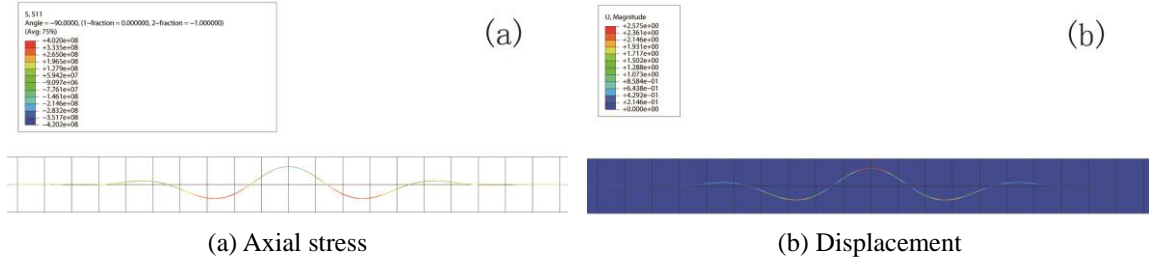
(a) Axial stress (b) Displacement

Fig. 6 Contour plot of the axial stress and displacement

(a) Temperature versus lateral displacement (b) Post-buckling forms
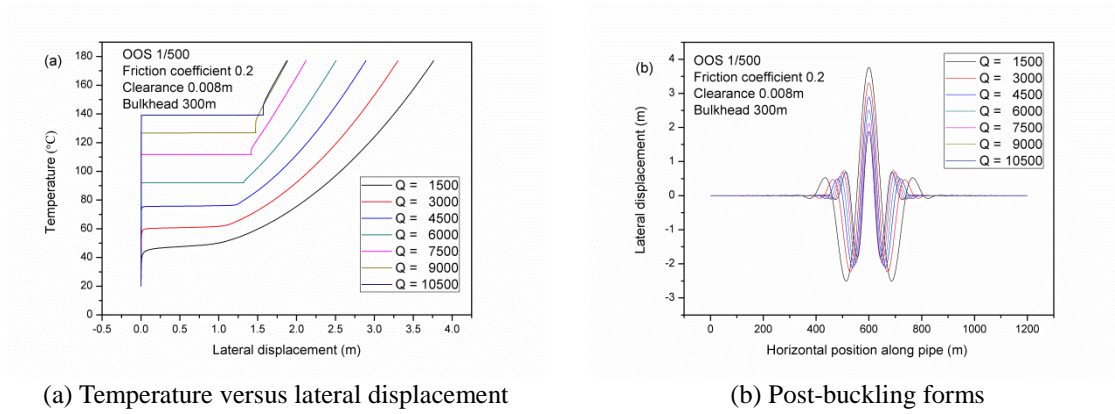
Fig. 7 Lateral buckling response with different submerged weight

Table 4 Geometric parameters of PIP pipeline

Items	Values						
Submerged weight Q (N/m)	1500	3000	4500	6000	7500	9000	10500
Critical temperature Tc (℃)	43.5	60.5	75.0	92.0	111.7	126.3	138.8
Critical axial force Fc (E+6N)	1.03	1.78	2.42	3.17	4.03	4.68	5.23

We called it Mode 5. A heavier submerged weight corresponds to a smaller buckled region and wavelength, and a smaller maximum lateral displacement. It is manifested that the post-buckling form is sensitive to the submerged weight.

4.2 Influence of imperfections

Previous research manifested the initial imperfection shape and OOS affect the upheaval buckling behavior (Hobbs 1984, Taylor and Gan 1986, Taylor and Tran 1993, Taylor and Tran 1996). Likewise, the initial imperfection shape and OOS also affect the lateral buckling behavior. In this study, we only consider the effect of OOS on the lateral buckling behavior. The effect of imperfection shape will be discussed in future work.
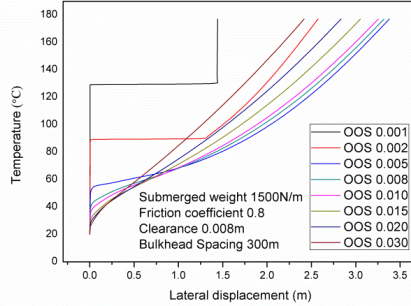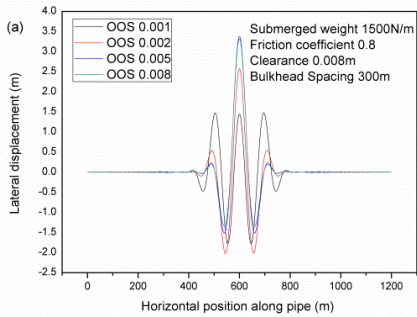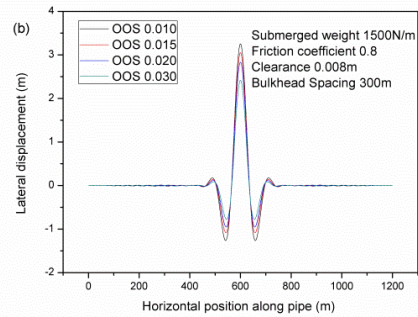
Fig. 8 Temperature-lateral displacement of mid-point of outer pipeline curves with different OOS

Table 5 The critical temperature and force with different OOS

Items	Values							
OOS	0.001	0.002	0.005	0.008	0.01	0.015	0.02	0.03
Critical temperature Tc (℃)	129.2	89.3	50.9	39.7	36	31.2	28.7	26.5
Critical axial force Fc (E+6N)	4.81	3.05	1.36	0.87	0.70	0.49	0.38	0.28

(a) OOS from0.001 to 0.008   (b) OOS from0.01 to 0.03

Fig. 9 Post-buckling forms with different OOS

The lateral buckling response of PIP pipelines with different OOS is shown in Fig.8. From this figure we know that a smaller the OOS of pipeline corresponds to a more evident of the "snap through" phenomenon and a higher critical temperature. The critical temperature and critical force is listed in Table 5. From Table 5, we know that the OOS of pipeline varying from 0.001 to 0.03, the critical force changes correspondingly from 4.81E+6 to 0.28E+6. Therefore, the OOS of pipeline also significantly influences the critical force.

The post-buckling form with different OOS is a little complicated which totally can be divided into two types, as shown in Fig. 9. When the OOS of pipeline is less than 0.01 (see Fig. 9(a)), the lateral buckling mode with different OOS of pipeline has seven half-wave and is developed from

Mode 5. We call it Mode 7. The lateral buckled region is not changed. For central lobe, a smaller OOS corresponds to a smaller final lateral displacement. While for the rest generated lobes flanking central lobe, the results are just opposite, that is, a smaller OOS corresponds to a larger final lateral displacement. Clearly, the "lobe extinction" phenomenon occurs.

When the OOS of pipeline is more than 0.01 (see Fig. 9(b)), the lateral buckling mode with different OOS of pipeline is Mode 5. The lateral buckled region is also not changed. The central and rest lobes have a consistent result that is, a smaller OOS corresponds to a larger final lateral displacement. The reason why this situation is different with above situations is that bifurcation happens only in the presence smaller OOS, which lead to the "lobe extinction" phenomenon. From above, it is clear that the lateral buckling is sensitive to the OOS of pipeline.

4.3 Influence of friction

The lateral buckling response of PIP pipelines with different lateral friction coefficient (isotropic) is shown in Fig. 10(a). From this figure, we can see that a larger lateral friction coefficient corresponds to a more evident of the "snap through" phenomenon and a higher the critical temperature. The critical temperature and critical force are listed in Table 6. From Table 6, we know that the lateral friction coefficient varies from 0.0 to 1.2, the critical force changes corresponding from 0.057E+6 to 4.66E+6. Therefore, the lateral friction coefficient of pipeline also significantly influences the critical force.

The lateral buckling response of PIP pipelines with anisotropy friction property and the comparison between that and related isotropic friction property is shown in Fig. 10(b). From this figure we can find out that axial friction coefficient doesn't affect the critical temperature or critical axial force, but does affect the post-buckling lateral displacement.

The post-buckling form with different lateral friction coefficient is more complicated. As shown in Fig. 11(a), when the lateral friction coefficient is in the range from 0.2 to 1.2, the lateral buckling mode is Mode 5. Moreover, a smaller lateral friction coefficient corresponds to larger lateral buckled region, and a larger lateral displacement.

(a) Friction with isotropic property   (b) Friction with anisotropy property
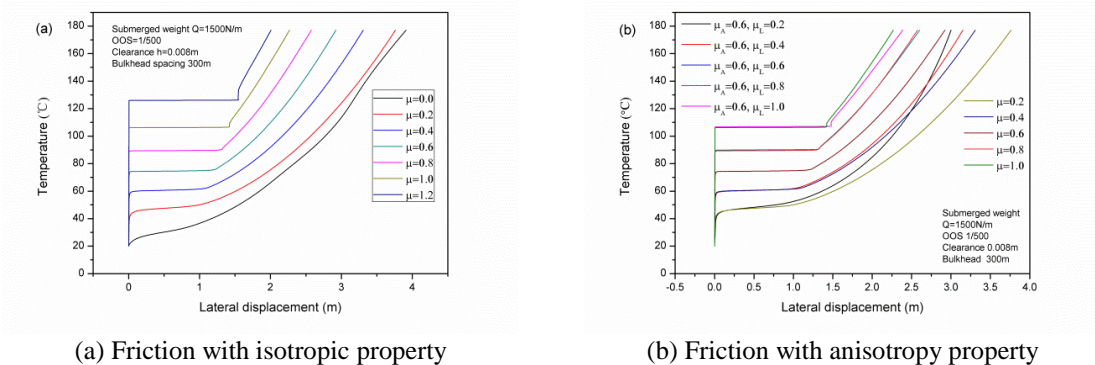
Fig. 10 Temperature versus lateral displacement with different friction coefficient

Table 6 The critical temperature and force with different lateral friction coefficient

Items	Values						
Lateral friction coefficient	0.0	0.2	0.4	0.6	0.8	1.0	1.2
Critical temperature Tc (℃)	21.3	39.8	56.6	72.7	88.9	106.0	125.9
Critical axial force Fc (E+6N)	0.057	0.87	1.61	2.32	3.03	3.79	4.66

(a) Lateral friction coefficient from 0 to 1.2   (b) Lateral friction coefficient from 0 to 0.1
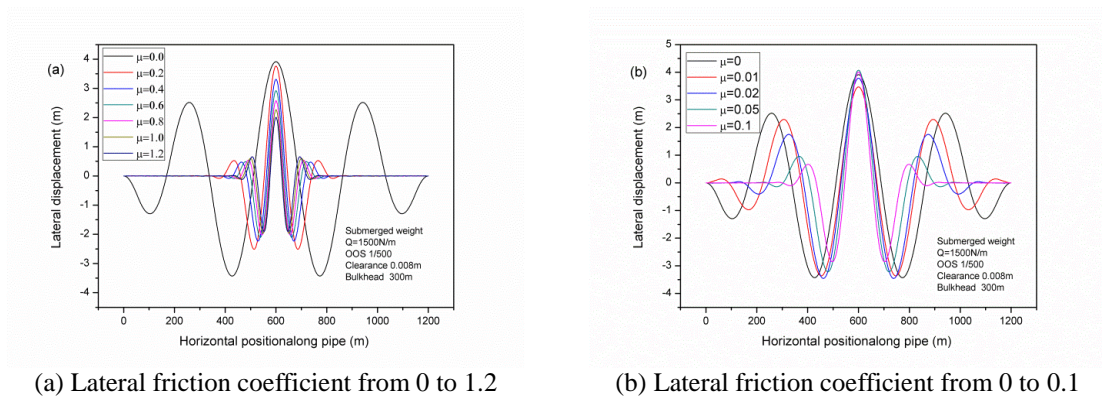
Fig. 11 Post-buckling forms with different lateral friction coefficient

Apparently, the buckling form with lateral friction coefficient 0 is very different with others. In order to see the evolutional process more clearly, an additional analysis was conducted where the lateral friction coefficient varying from 0.0 to 0.1. The results are shown in Fig. 11(b). When the lateral friction coefficient is in the range from 0.0 to 0.1, more lobes appear and the length and amplitude of lobes are all decreased with the increasing of lateral friction coefficient. The amplitudes and wavelengths of lobes are decayed from middle to two sides. The lateral buckled regions are also decayed with the increasing of lateral friction coefficient.
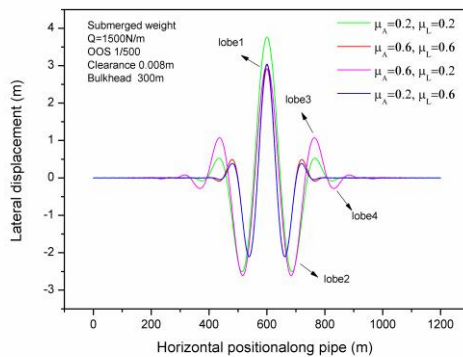

Fig. 12 Post-buckling forms with anisotropy friction property

The post-buckling forms with anisotropy friction property are shown in Fig. 12. If we put two and two together, we can find out that the axial friction coefficient affects the amplitudes of lobes and feed-in response, but doesn't affect the wavelengths of lobes. While, the lateral friction coefficient affects the lengths and amplitudes of other lobes except the central lobe (lobe 1). This may be because of the phenomenon of "Lobe-extinction" of central lobe has occurs, while other lobes are growing when temperature reached to 177℃ (Miles 1999). The ratio of axial friction coefficient and lateral friction coefficient also affects the response of lateral buckling.

4.4 Influence of clearance

The clearance is an important structural parameter of PIP pipelines. The lateral buckling response of PIP pipelines with different clearance between the inner and outer pipe is shown in Fig. 13. As illustrated in Fig. 14, a smaller clearance corresponds to a higher critical temperature. But different from other parameters, the clearance doesn't affect the degree of evident of the "snap through" phenomenon. The critical temperature and critical force is listed in Table 7.

From Table 7, we know that the clearance between inner pipe and outer pipe varies from 0.001 to 0.048, the critical force changes correspondingly from 3.29E+6 to 2.48E+6. Therefore, the clearance of pipeline also significantly influences the critical force.

The post-buckling forms with different clearance are more complicated. Totally, they can be divided into two types. As shown in Fig. 14(a), when the clearance is in the range from 0.001 to 0.024, the lateral buckling modes are all Mode 5. While, when the clearance is in the range from 0.024 to 0.048, the lateral buckling forms display very different, as shown in Fig. 14(b).
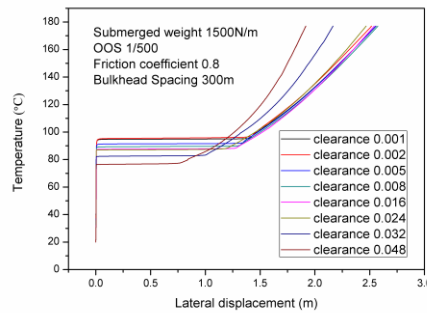

Fig. 13 Temperature-lateral displacement of mid-point of outer pipeline curves with different clearance

Table 7 The critical temperature and force with different OOS

Items	Values							
Clearance	0.001	0.002	0.005	0.008	0.016	0.024	0.032	0.048
Critical temperature Tc (℃)	94.7	93.6	90.6	88.8	87.4	87.0	82.3	76.4
Critical axial force Fc (E+6N)	3.29	3.24	3.11	3.03	2.97	2.95	2.74	2.48

(a) Clearance from 0.001 to 0.024   (b) Clearance from 0.024 to 0.048

Fig. 14 Post-buckling forms with different clearance

(a) Temperature versus lateral displacement   (b) Post-buckling forms
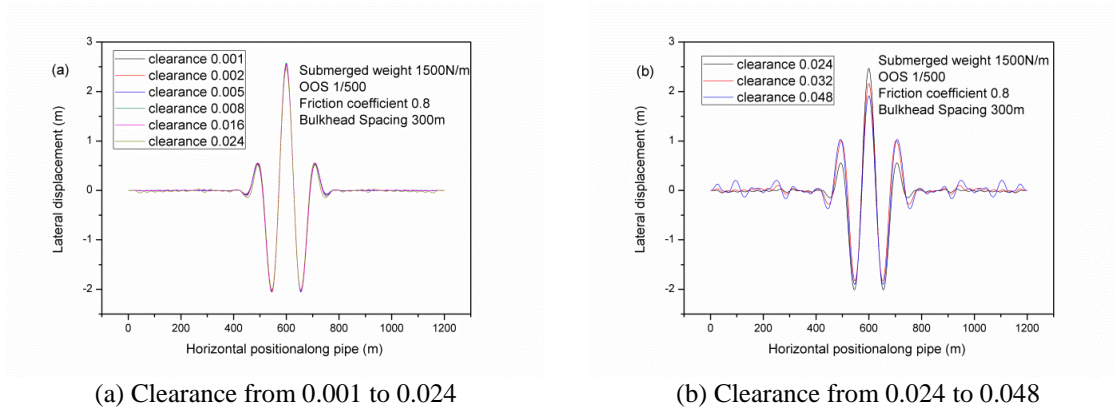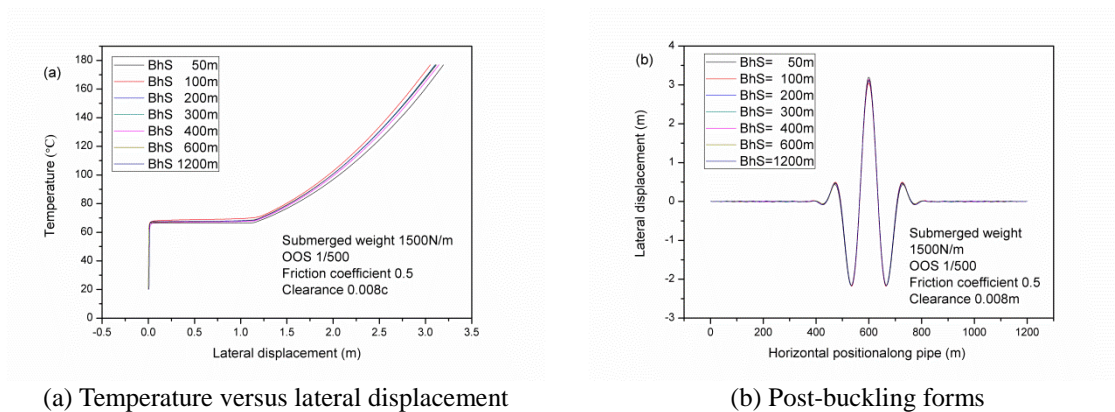
Fig. 15 Lateral buckling response with different bulkhead spacing

With the increasing of clearance, the number and amplitude of lobes also increase. The reason why it will produce these two different results maybe is that oversize clearance leads to oversize contact stress between inner and outer pipe, and the localization of buckling can't release enough force, then the rest region buckles. The difference of inner radius of outer pipe and outer radius of inner pipe is 0.053 which is almost twice the value of turning point 0.024. So we can get a conclusion that the turning phenomenon of post-buckling forms will be happen. When the clearance is in the range from 0 to turning point, the post-buckling forms are not sensitive to clearance, while, the clearance is above the turning point the post-buckling forms are sensitive to clearance. The value of turning point is approximate to half of the difference of inner radius of outer pipe and outer radius of inner pipe.

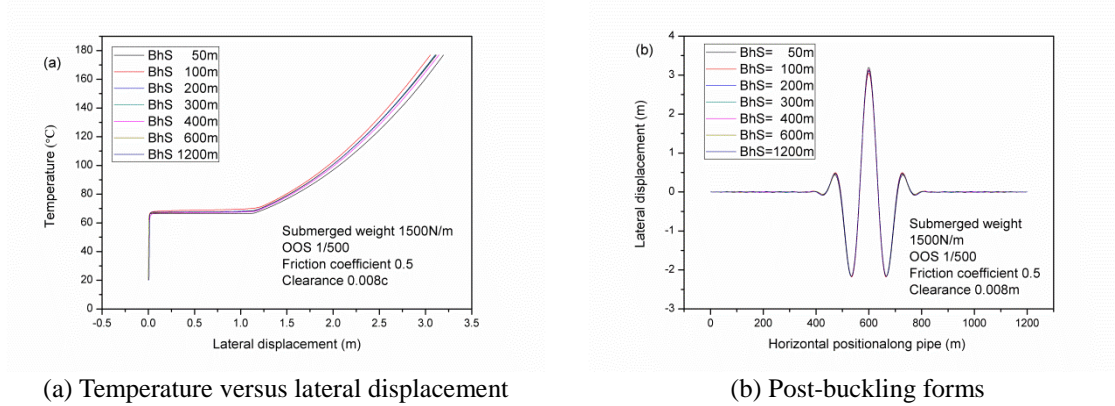(a) Temperature versus lateral displacement   (b) Post-buckling forms

Fig. 15 Lateral buckling response with different bulkhead spacing
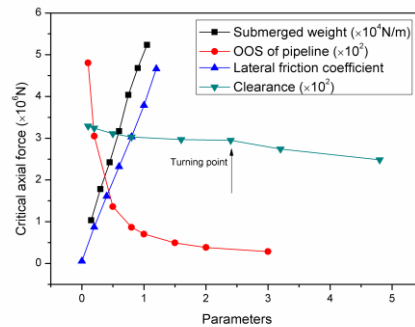

Fig. 16 The relationship between critical force and these four parameters including submerged weight, OOS of pipelines, lateral friction coefficient and clearance.

4.5 Influence of bulkhead spacing

The bulkhead spacing is also an important structural parameter of PIP pipelines. The lateral buckling response of PIP pipelines with different bulkhead spacing is shown in Fig. 15. From Fig. 15(a) we know that with the increasing of bulkhead spacing from 50 m to 1200 m, the critical temperatures do not change. The maximum lateral buckling displace with different bulkhead spacing when the temperature reached to 177 ℃ has little difference. This manifests that the critical force of lateral buckling is not sensitive to bulkhead spacing.

The post-buckling forms with different bulkhead spacing are shown in Fig. 15(b). We can see that the lateral buckling forms with different bulkhead spacing are all Mode 5. This manifests that the lateral post-buckling form is also not sensitive to bulkhead spacing.

From above, we know that the lateral buckling critical force is sensitive to these parameters including submerged weight, OOS of pipelines, lateral friction coefficient and clearance. The bulkhead spacing almost doesn't affect the behaviors of lateral buckling including critical force

and post-buckling response. The relationships between critical force and these parameters are shown in Fig. 16. It is suggested that there exist two positive correlations between critical axial force and submerged weight and between critical axial force and lateral critical coefficient. However, there also exist two negative correlations between critical axial force and OOS of pipeline and between critical axial force and clearance. Meanwhile, there exists a turning point in the relationship curve between critical axial force and clearance where the relationship between critical axial force and clearance changed. The lateral buckling forms are mainly observed to be Mode 5 or its evolution which represented the lowest energy configuration.

5. Conclusions

Structural based finite element modeling procedures have been developed to investigate a range of parameters on the lateral buckling response of PIP system. The parameters included the submerged weights, OOS of pipeline, lateral friction coefficient between pipelines and seabed, clearance between the outer pipe and inner pipe and bulkhead spacing.

The lateral buckling critical force is affected by these parameters including submerged weights, OOS of pipeline, lateral friction coefficient and clearance. Two of them submerged weights and lateral friction coefficient have a positive correlation to the critical axial force. While, the others parameters OOS of pipelines and clearance have a negative correlation to the critical axial force. There exists a turning point in the relationship curve between critical force and clearance where the relationship between critical force and clearance changed.

Future work will focus on refining the modeling procedures to incorporate pipe/soil nonlinear interaction model (for example vertical penetration, lateral and axial force-displacement relationships, *et al*.). The parameter study will investigate other factors that include imperfection shape, seabed topography and installation residual forces, *et al*.

Acknowledgments

References

ABAQUS 6.14 Analysis User's Guide. (2014), Volume IV: Elements.

Global buckling of submarine pipelines—Structural design due to high temperature/high pressure (2007), DNV RP-F110.

Haq, M.M. and Kenny, S. (2014), "Assessment of parameters influencing lateral buckling of deep subsea Pipe-in-Pipe pipelines system using Finite Element Method", *Proceedings of the ASME 2014 33rd International Conference on Ocean, Offshore and Arctic Engineering*, San Francisco, California, USA, June.

Haq, M.M. and Kenny, S. (2013), "Lateral buckling response of subsea HTHP pipelines using Finite Element Methods", *Proceedings of the ASME 2013 32nd International Conference on Ocean, Offshore and Arctic Engineering*, Nantes, France, June.

Harrison, G.E., Kershenbaum, N.Y. and Choi, H.S. (1997), "Expansion analysis of subsea pipe-in-pipe flowline", *Proceedings of the 7th (1997) International Society of Offshore and Polar Engineers*, Honolulu, Hawaii, USA, January.

He, T., Duan, M.L. and An, C. (2014), "Prediction of the collapse pressure for thick-walled pipes under external pressure , *Appl. Ocean Res.*, **47**, 199-203.

Hobbs, R.E. (1984), "In-service buckling of heated pipelines", *J. Transp. Eng. -ASCE*, **110**(2), 175-189.

Jukes, P., Eltaher, A., Sun, J. and Harrison. G. (2009), "Extra high-pressure high-temperature (XHPHT) flowlines: design considerations and challenges", *Proceeding of the ASME 2009 28th International Conference on Ocean, Offshore and Arctic Engineering*, Honolulu, Hawaii, USA, May.

Karampour, H., Albermani, F. and Gross, J. (2013), "On lateral and upheaval buckling of subsea pipelines," *Eng. Struct.*, **52**, 317-330.

Kershenbaum, N.Y., Harrison, G.E. and Choi, H.S. (1996), "Subsea pipeline lateral deviation due to high temperature product", *Proceedings of the 6th (1996) - International Offshore and Polar Engineering Conference*, Los Angeles, USA, May.

Miles, D.J. and Calladine, C.R. (1999), "Lateral thermal buckling of pipelines on the sea bed", *J. Appl. Mech. - ASCE*, **66**(4), 891-897.

Palmer, A.C. and Baldry, J.A.S. (1974), "Lateral buckling of axially constrained pipelines", *J. Petroleum Technol.*, **26**(11), 1283-1284.

Palmer, A.C., Ellinas, C.P. and Richards, D.M. and Guijt, J. (1990), "Design of submarine pipelines against upheaval buckling", *Proceeding of the Offshore Technology Conference*, Houston, Tesas, USA, May.

Rong, H., Inglis, R., Bell, G., Huang, Z. and Chan, R. (2009), "Evaluation and mitigation of axial walking with a focus on deep water flowlines", *Proceeding of the Offshore Technology Conference*, Houston, Tesas, USA, May.

Soreide, T., Kvarme, S.O. and Paulsen, G. (2005), "Pipeline expansion on uneven seabed", *Proceedings of the 15th (2005) International Offshore and Polar Engineering Conference*, Seoul, Korea, June.

Submarine Pipeline Systems (2012), DNV OS-F101.

Taylor, N. and Gan, A.B. (1986), "Submarine pipeline buckling-imperfection studies", *Thin Wall. Struct.*, **4**(4), 295-323.

Taylor, N. and Tran, V. (1993), "Prop-imperfection subsea pipeline buckling", *Mar. Struct.*, **6**(4), 325-358.

Taylor, N. and Tran, V. (1996), "Experimental and theoretical studies in subsea pipeline buckling", *Mar. Struct.*, **9**(2), 211-257.

Vaz, M.A. and Patel, M.H. (1999), "Lateral buckling of bundled pipe systems", *Mar. Struct.*, **12**(1), 21-40.

Zhang, X. and Duan, M. (2015), "Prediction of the upheaval buckling critical force for imperfect submarine pipelines", *Ocean Eng.*, **109**, 330-343.